Interaction of Pyrene-Labeled Hydrophobically Modified Polyelectrolytes with Oppositely Charged Mixed Micelles Studied by Fluorescence Quenching

Masanobu Mizusaki and Yotaro Morishima*

Department of Macromolecular Science, Osaka University, Toyonaka, Osaka, 560 Japan

Paul L. Dubin

Department of Chemistry, Indiana University−Purdue University, Indianapolis, Indiana 46205-2820

Received: October 2, 1997; In Final Form: December 10, 1997

Pyrene-labeled hydrophobically modified polyanions were prepared by terpolymerization of sodium 2-(acrylamido)-2-methylpropanesulfonate, *N*-dodecylmethacrylamide (2.5−7.5 mol %), and *N*-(1-pyrenylmethyl)methacrylamide (1 mol %). Dynamic interactions of these polymers with mixed micelles of *n*-dodecyl hexa(oxyethylene) glycol monoether ($C_{12}E_6$), cetyltrimethylammonium chloride (CTAC), and cetylpyridinium chloride (CPC) (quencher for pyrene fluorescence) were monitored by fluorescence quenching. The charge on the micelle was varied systematically by varying the mole fraction of CTAC (Y) in the mixed micelle. All quenching experiments were performed at $Y < Y_p$, where Y_p is a critical Y at which the polymer−micelle systems undergo macroscopic phase separation. A kinetic model was developed to estimate the binding constant (K) (where $K = k_1/k_{-1}$), association rate constant (k_1), and lifetime of bound micelle on the polymer (residence time) ($1/k_{-1}$) from steady-state and time-dependent fluorescence-quenching data. This analysis led to the following results: K increases with Y because both k_1 and $1/k_{-1}$ increase with Y, k_1 being more dependent on Y than $1/k_{-1}$. K markedly increases with increasing concentration of dodecyl groups in the polymers, even at small Y, indicating a strong enhancement of polymer−micelle interactions by hydrophobic interactions. This large increase in the binding constant arises mainly from a large increase in the residence time with increase in the hydrophobe content in the polymers, $1/k_{-1}$ being much more dependent on the hydrophobe content than k_1. The results indicate that complex formation results from hydrophobic interactions between dodecyl groups and the micelle superimposed on the effect of electrostatic force.

Introduction

Polyelectrolytes interact strongly with oppositely charged mixed micelles of ionic/nonionic surfactants, normally leading to phase separation. These coacervation or precipitation phenomena are related to the phase separation observed for mixtures of oppositely charged polyelectrolytes[1] and arise from the electrostatic attraction of the two macroions, leading to the displacement of microions and the concomitant loss of hydration. However, just as polyelectrolytes of low or highly asymmetric linear charge densities may form soluble complexes, polyelectrolyte−micelle complexes may form stable, equilibrium molecular species if the electrostatic attractions are attenuated by proper adjustment of the polyion linear charge density (ξ), the micelle surface charge density (σ), or the ionic strength (I). Under these conditions, soluble complexes with dimensions between 1 and 10 times those of the polyelectrolyte may be formed.

There are two distinct reasons for interest in such systems. First, these soluble polymer−micelle complexes may be investigated by a huge range of experimental methods, including turbidimetry,[2−5] dynamic and static light scattering,[6−10] viscometry,[10,11] electrophoretic light scattering,[10] microcalorimetry,[12] dye solubilization,[13,14] and equilibrium dialysis.[6,15,16] Such studies provide information about the way in which somewhat organized structures can arise in purely synthetic systems by a combination of electrostatic and hydrophobic interactions. Second, despite their dynamic nature, micelles can be viewed as models for small charged colloidal particles, inasmuch as their interaction with polyelectrolytes is controlled by micelle charge density and geometry. Thus, the interaction of micelles with oppositely charged polyelectrolytes strongly resembles the interaction of those same polyelectrolytes with other particles of similar size and charge, for example, proteins[17] and dendrimers.[18] In all these cases, complex formation occurs when σ reaches an adequate level, and the magnitude of this value varies directly with $I^{1/2}$ and inversely with ξ. The appearance of the complexed state is sufficiently abrupt to enable the identification of a critical surface charge density (σ_{crit}) so that the foregoing observations may be expressed as

$$\sigma_{crit} \approx \xi^{-1}\kappa^{a} \qquad (1)$$

where κ is the Debye−Hückel parameter. The observation of such phase-transition-like behavior is consistent with theoretical predictions for the interaction of polyelectrolytes with oppositely charged flat,[19−21] cylindrical,[22] or spherical[23] surfaces and with more recent simulations.[24] These results are also relevant to efforts directed toward analytical solutions for the electrostatics of DNA−protein association.[25]

Despite the range of studies applied to such systems, little is known about the dynamics of the polyelectrolyte−micelle interaction. The simulations noted above[24] suggest that transient interactions take place prior to the appearance of a "bound"

S1089-5647(97)03211-2 CCC: $15.00
Published on Web 02/20/1998

SCHEME 1

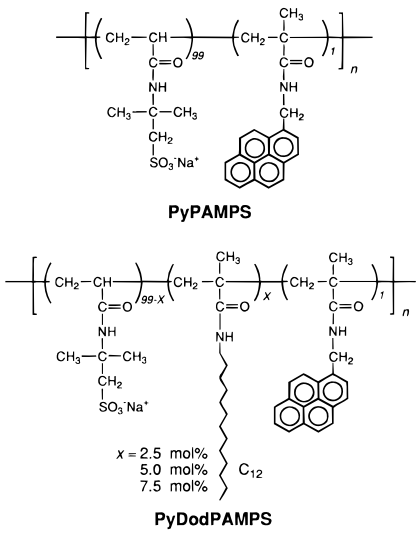

colloid state ("prior to" in the sense of "at a higher ionic strength", but "at a lower colloid surface charge density" would be equivalent); however, no experimental verification of such predictions exists. Fluorescence techniques offer, in principle, considerable insight into such questions.[26,27] Although fluorescence probes have been frequently used to study polymer−surfactant interactions,[28] the goal of such investigations has been the determination of the aggregation number of bound (i.e., versus free) micelles. A different application of fluorescence to polyelectrolyte−colloid interactions was presented in our investigation of the fluorescence behavior of a pyrene-tagged polyanion arising from its photophysical interaction with tryptophan residues in lysozyme.[29] More recently, we used a similar polymer in conjunction with quencher-carrying mixed micelles to characterize the microscopic polyelectrolyte−micelle phase transition.[26,27] The intensity of the polyelectrolyte−micelle interaction in such systems may be modulated in two ways: by controlling the ratio of cationic to nonionic surfactants in the micelle (i.e., σ) and by controlling the ionic strength (i.e., κ). The enhancement of quenching upon increase in σ or decrease in κ was investigated by steady-state and time-dependent fluorescence spectroscopy to provide insight into the dynamics of polyelectrolyte−micelle association.[26,27]

The behavior of fluorescence-labeled polyelectrolytes may be perturbed by the physicochemical properties of the label. Thus, turbidimetric, light scattering, and fluorescence studies revealed that the interaction of pyrene-labeled poly(sodium 2-(acrylamido)-2-methylpropanesulfonate) (PAMPS) with mixed micelles of *n*-dodecyl hexa(oxyethylene) glycol monoether ($C_{12}E_6$) and cetyltrimethylammonium chloride (CTAC), although predominantly driven by electrostatic forces, occurred preferentially with pyrene sites.[26] Thus, we observed a conjoint effect of hydrophobic and electrostatic interactions on the polyion−micelle interaction.[26,27]

One aspect of the present work is the resolution of electrostatic and hydrophobic contributions to the binding of micelles to polyelectrolytes. As noted, fluorescence-quenching studies can yield substantial insight into the thermodynamics and kinetics of polyelectrolyte−micelle association. However, since the binding that is studied takes place at the fluorophore itself, its hydrophobic contribution is difficult to isolate. To control hydrophobic contributions in a more systematic way, we have incorporated variable amounts of *n*-dodecyl side chains into pyrene-labeled PAMPS (Scheme 1). Since the pyrene groups in PyPAMPS (Scheme 1) have a rather modest hydrophobic interaction with micelles, penetrating only into the ethylene oxide corona,[26,27] it is useful to observe the influence of a more effective hydrophobe.

The growing interest in hydrophobically modified water-soluble polymers[30] encompasses their interactions with surfactants[31−33] and proteins.[34] A fundamental consideration is the competition between intrapolymer association (intramolecular micellization) and intermolecular hydrophobic interactions (between polymer hydrophobes and the cosolute). Intrapolymer micelles could provide a solubilizing environment for the cosolute. On the other hand, intramolecular micellization could make polymer hydrophobes less available for interaction with another molecule. In the present case, polymer-bound pyrene may be used as a probe to monitor the dependence of polymer−micelle interaction on the polymer hydrophobe concentration and so to distinguish between these two scenarios.

In this work, we employed pyrene-labeled hydrophobically modified PAMPS (PyDodPAMPS shown in Scheme 1) and $C_{12}E_6$/CTAC mixed micelles in which cetylpyridinium chloride (CPC) was solubilized. Polymer−micelle interactions were monitored by steady-state and time-dependent fluorescence quenching. A kinetic model, based on an association equilibrium, allowed us to estimate the binding constant, residence time, and association rate constant from quenching data.

Experimental Section

Materials. Pyrene-labeled hydrophobically modified polyanions were prepared by terpolymerization of sodium 2-(acrylamido)-2-methylpropanesulfonate (AMPS), *N*-dodecylmethacrylamide (DodMAm), and *N*-(1-pyrenylmethyl)methacrylamide (PyMAm) according to a method reported previously.[35] The contents of dodecyl groups in the terpolymers were 2.5, 5, and 7.5 mol %. A copolymer of AMPS and PyMAm was also prepared as previously described.[35] The content of pyrene units in the co- and terpolymers was 1 mol %, which was determined by UV absorbance at 343 nm.

$C_{12}E_6$ (Nikko Chemical) was used without further purification. CTAC and CPC (both form Wako Pure Chemicals) were recrystallized twice from methanol. Milli-Q water was used for fluorescence measurements and turbidimetric titration.

Fluorescence. Steady-state fluorescence spectra were recorded on a Hitachi F-4500 fluorescence spectrophotometer with excitation at 343 nm. To prepare a CPC-bearing $C_{12}E_6$ micelle stock solution, a mixture of 0.5 mM CPC, 30 mM $C_{12}E_6$, and a predetermined concentration of NaCl was stirred overnight. For "type I" fluorescence titration,[26,27] a solution of 50 mM CTAC in a predetermined concentration of NaCl was added to a mixture of 0.05 g/L polymer and the CPC-solubilized $C_{12}E_6$ stock solutions at a constant ionic strength.

Fluorescence decays were measured by a time-correlated single-photon-counting technique using a Horiba NAES 550 system. Decay curves were analyzed by a conventional deconvolution technique. Sample solutions were the same as those used for the steady-state fluorescence measurements.

Turbidimetric Titration. Turbidimetric titrations were carried out at 420 nm with a JASCO V-520 spectrophotometer with a 1-cm path-length quartz cuvette. Type I turbidimetric titrations[2−5,36,37] were performed at 25 ± 1 °C by adding a solution of 50 mM CTAC to a mixture of 0.05 g/L polymer, 30 mM $C_{12}E_6$, and 0.5 mM CPC at a constant ionic strength. The ionic strengths were adjusted with NaCl. All transmittance values were corrected by subtracting the turbidity of a polymer-

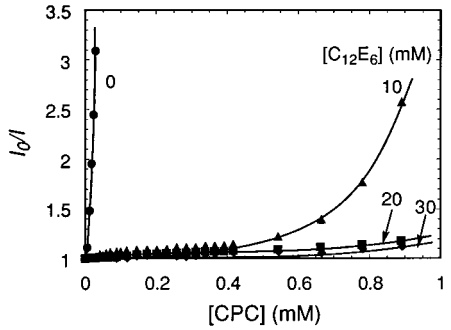

Figure 1. Stern−Volmer plots for fluorescence quenching of PyPAMPS by CPC in the absence and presence of varying concentrations of $C_{12}E_6$ in 0.2 M NaCl aqueous solution.

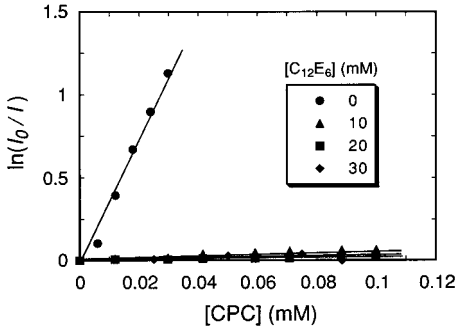

Figure 2. Perrin plots for fluorescence quenching of PyPAMPS by CPC in the absence and presence of varying concentrations of $C_{12}E_6$ in 0.2 M NaCl aqueous solution.

free blank. The blank-corrected turbidity (100% − transmittance) was plotted as a function of *Y*, the mole fraction of the cationic surfactant in the mixed micelle, defined as $Y = ([CTAC] + [CPC])/([CTAC] + [CPC] + [C_{12}E_6])$.

Quasielastic Light Scattering (QELS). QELS was carried out at a scattering angle of $\theta = 90°$ with an Otsuka Electronics Photal DLS-7000 light-scattering spectrometer equipped with a 75-mW Ar laser. All QELS measurements were performed at 25 °C. Sample solutions were filtered with a 0.2-μm membrane filter prior to measurement. Correlation functions were analyzed by a histogram method and used to determine the diffusion coefficient (*D*) of samples. *D* was converted into the hydrodynamic radius (R_h) using the Stokes−Einstein equation, $R_H = k_BT/(6\pi\eta D)$, where k_B is the Boltzmann constant, *T* is the absolute temperature, and η is the solvent viscosity.

Results

Fluorescence Quenching by Free CPC. Pyrene fluorescence is known to be quenched by CPC.[38] Figure 1 compares Stern−Volmer plots for fluorescence quenching of pyrene-labeled polyAMPS (PyPAMPS) (Scheme 1) by CPC in the absence and presence of varying concentrations of $C_{12}E_6$ at $I = 0.2$. Here, I_0 and *I* are the steady-state fluorescence intensities in the absence and presence of CPC, respectively. In the absence of $C_{12}E_6$, the quenching with CPC is highly efficient. Time-dependent fluorescence quenching shows no decrease in fluorescence lifetime with an increase in the CPC concentration but merely a decrease in the fluorescence peak intensity (peak count in a single-photon-counting measurement of fluorescence decays). This indicates that CPC, a cationic quencher, binds closely to pyrene sites in the polyanion and that the quenching occurs extremely rapidly, compared to the fluorescence lifetime, in a static mechanism. In fact, the steady-state-quenching data follow the Perrin kinetics[39] as shown in Figure 2. However, in the presence of micellar $C_{12}E_6$ (cmc for $C_{12}E_6$ is 0.06 mM at 20 °C [40]), the quenching is remarkably suppressed (Figures 1 and 2). This indicates that CPC molecules are solubilized in $C_{12}E_6$ micelles, and direct interaction with PyPAMPS is prevented. As the concentration of $C_{12}E_6$ decreases, the molar ratio CPC/$C_{12}E_6$ increases and the positive charge density of the CPC-carrying micelle increases, allowing the micelle to interact electrostatically with the polyanion. Thus, significant quenching is observed for [CPC] ≅ 0.8 mM in the presence of 10 mM $C_{12}E_6$, corresponding to a cationic mole fraction of 0.075, consistent with the mole fraction of cationic surfactant in the mixed micelle (*Y*) required for substantial quenching in the CTAC/$C_{12}E_6$ system (see below).

Fluorescence Quenching with CPC-Carrying Micelles. To study the interactions of pyrene-labeled polymers with CPC-carrying $C_{12}E_6$/CTAC mixed micelles, we employed constant concentrations of 0.5 mM CPC and 30 mM $C_{12}E_6$. At these conditions practically all CPC molecules are solubilized in the micelles (Figure 1), giving an average number of CPC per micelle of about 5, assuming the aggregation number of $C_{12}E_6$ to be 3×10^2.[40]

The micelle charge density can be continuously increased by a "type I" titration,[26,27] which involves the addition of CTAC to CPC-carrying $C_{12}E_6$ micelles. Figure 3 compares fluorescence spectra of PyPAMPS and PyDodPAMPS with various dodecyl contents (Scheme 1) in the presence of 30 mM $C_{12}E_6$ at $I = 0.2$ with and without 0.5 mM CPC at varying *Y*, where $Y = \{[CTAC] + [CPC]\}/\{[C_{12}E_6] + [CTAC] + [CPC]\}$. Under these conditions, the contribution of CPC to *Y* is 0.016. Fluorescence of PyPAMPS is only slightly quenched at $Y < 0.04$, owing to dynamic quenching arising from collisional encounters of CPC-carrying micelles with pyrene sites in PyPAMPS, as indicated by single-exponential decays of pyrene fluorescence at $Y \leq 0.04$ (Figure 4).[27] These observations, taken together with the results in Figure 1, indicate that essentially all CPC molecules are incorporated into the micelles and that no free CPC remains in the bulk-water phase. At $Y \cong 0.05$, however, fluorescence quenching of PyPAMPS begins to increase significantly with *Y* and fluorescence decay becomes a double-exponential with a shorter lifetime component on the order of 50 ns (Figure 4). This value corresponds to a critical *Y* value (Y_c), corresponding to the critical micelle charge density σ_{crit} in eq 1, at which soluble polymer−micelle complexes are formed.[26,27] Fluorescence of PyPAMPS is strongly quenched in the region $Y > Y_c$, exhibiting double-exponential decays, up to the occurrence of macroscopic phase separation at $Y = Y_p$. At $Y \leq 0.04$, PyPAMPS and micelles encounter each other by collisions and the residence time of the micelles in the collision complex may be much shorter than the lifetime of pyrene fluorescence. At $Y \geq 0.05$, however, an association complex can form in which the micelle residence time may be comparable to or longer than the lifetime of pyrene fluorescence, as will be discussed later in detail.

In the case of hydrophobically modified polymers, by contrast, fluorescence is strongly quenched and the fluorescence decays are double-exponential even at $Y = 0.02$. With an increase in the dodecyl content in PyDodPAMPS, the regime of the strong quenching is observed at smaller *Y* values. The extent of quenching at $Y = 0.02$ increases with increasing dodecyl content in PyDodPAMPS. The quenching is increased by an increase in *Y*, but the effect of *Y* on the quenching becomes less when the dodecyl content is increased.

Figure 5 compares type I turbidimetric titration and fluorescence-quenching data for PyPAMPS and PyDodPAMPS at *I*

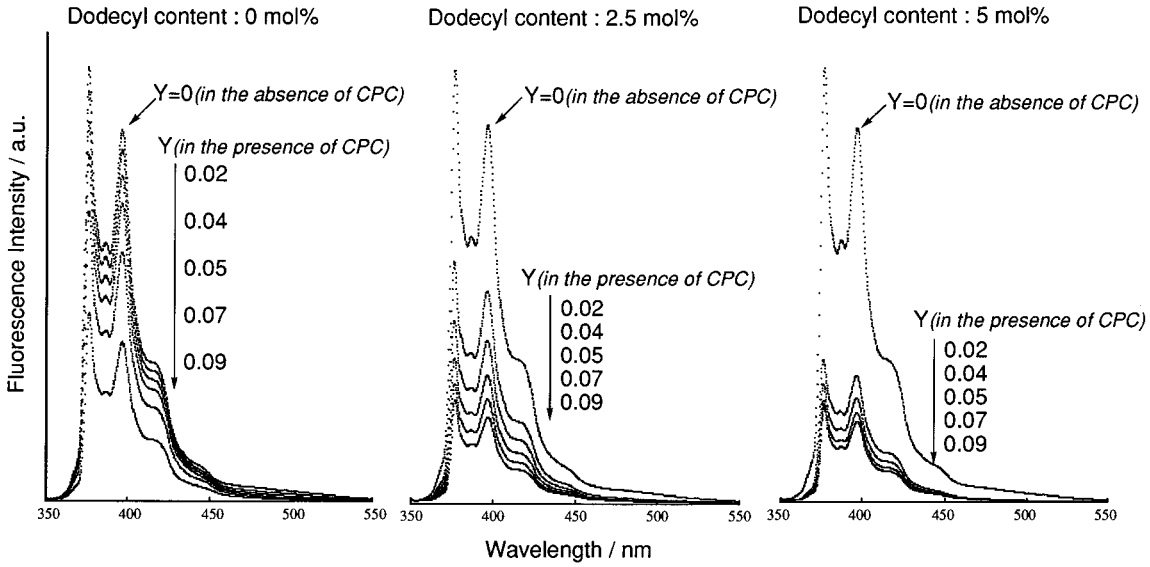

Figure 3. Steady-state fluorescence spectra for PyPAMPS and PyDodPAMPS at varying Y in the absence and presence of CPC-carrying $C_{12}E_6$/CTAC mixed micelles: [polymer] = 0.05 g/L, [$C_{12}E_6$] = 30 mM, [CPC] = 0.5 mM, and [NaCl] = 0.2 M.

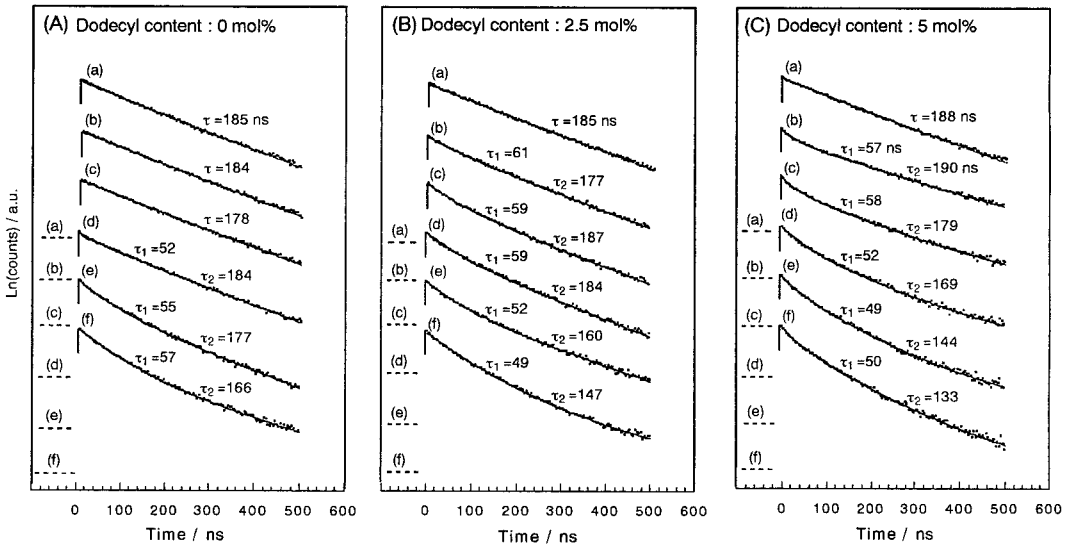

Figure 4. Fluorescence-decay profiles for PyPAMPS (A), PyDodPAMPS with 2.5 mol % dodecyl content (B), and PyDodPAMPS with 5 mol % dodecyl content (C) in [NaCl] = 0.2 M at varying Y: (a) $Y = 0$; (b) $Y = 0.02$; (c) $Y = 0.04$; (d) $Y = 0.05$; (e) $Y = 0.07$; (f) $Y = 0.09$. For $Y = 0$, [polymer] = 0.05 g/L and [$C_{12}E_6$] = 30 mM without CPC. For $Y = 0.02-0.09$, [polymer] = 0.05 g/L, [$C_{12}E_6$] = 30 mM, and [CPC] = 0.5 mM. The baseline for each decay curve is indicated by a broken line. The best-fit curves from use of a double-exponential function are indicated in the figure (decays for PyPAMPS at $Y = 0$, 0.02, and 0.04 and for PyDodPAMPS at $Y = 0$ are single-exponential). Lifetimes obtained from the best-fit curves are also indicated in the figure.

= 0.2. As can be seen in Figure 5a, macroscopic phase separation occurs near $Y = 0.15$; PyDodPAMPS exhibits Y_p slightly lower than that of PyPAMPS. In Figure 5b, the normalized fluorescence intensities, I/I_0, are plotted as a function of Y at $I = 0.2$, where I is the fluorescence intensity for the pyrene-labeled polymers in the presence of CPC-carrying $C_{12}E_6$/CTAC micelles at varying Y, and I_0 is the fluorescence intensity in the presence of CPC-free micelles at $Y = 0$. Strong quenching occurs at $Y < Y_p$, which provides evidence of binding between the pyrene-labeled polymers and CPC-carrying micelles at $Y < Y_p$. For dodecyl-containing polymers, strong quenching occurs at $Y \cong 0$, and no Y_c is recognized. The extent of quenching at $Y \cong 0$ increases with increasing dodecyl content and the quenching is increased by an increase in Y, the quenching being less dependent on Y at higher dodecyl contents. These observations indicate that polymer−micelle association can take place solely through hydrophobic interactions of the polymer-bound dodecyl groups with micelles at $Y \cong 0$. However, polymer−micelle association is enhanced by conjoint electrostatic interactions, which are more significant for polymers with lower dodecyl contents.

Kinetic Analysis

To quantitatively interpret the fluorescence-quenching data, we propose a simple kinetic model based on an association equilibrium for pyrene-labeled polymers and CPC-carrying $C_{12}E_6$/CTAC mixed micelles (Scheme 2). In Scheme 2, P denotes the pyrene site in the polymer, M the quencher-carrying mixed micelle, PM the complex between P and M, k_1 and k_{-1} the association and dissociation rate constants, respectively, τ_0 the fluorescence lifetime of pyrene in the absence of the

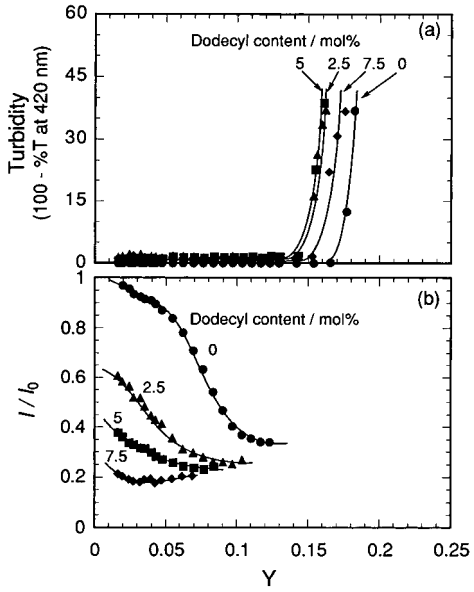

Figure 5. Comparison of turbidity (a) and normalized fluorescence intensity (b) for PyPAMPS and PyDodPAMPS as a function of *Y*: [polymer] = 0.05 g/L, [$C_{12}E_6$] = 30 mM, [CPC] = 0.5 mM, and [NaCl] = 0.2.

SCHEME 2

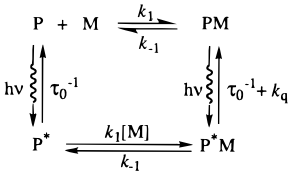

quencher, and k_q the first-order quenching rate constant within the complex. At equilibrium, the concentration of the complex is given by

$$[PM] = K[P][M] \tag{2}$$

where K is the association equilibrium constant (binding constant), that is, $K = k_1/k_{-1}$.

When the system is irradiated with UV light at equilibrium, both free (uncomplexed) and complexed pyrene chromophores are photoexcited. Fluorescence quenching occurs within the complex, but photoexcited free pyrene (P*) can encounter quencher-carrying mixed micelles within its lifetime and can form a complex (P*M) with the rate constant k_1.

Assuming that the rate of deactivation of singlet-excited pyrene in the complex is much faster than the rate of dissociation of the complex, that is, $\tau_0^{-1} + k_q \gg k_{-1}$, one can derive the rate equations for [P*] and [P*M] under transient conditions with excitation at time $t = 0$ by a light pulse of negligible duration:

$$d[P^*]_t/dt = -(\tau_0^{-1} + k_1[M])[P^*]_t \tag{3}$$

$$d[P^*M]_t/dt = -(\tau_0^{-1} + k_q)[P^*M]_t + k_1[P^*]_t[M] \tag{4}$$

When eqs 3 and 4 are solved and the initial condition $[P^*] = [P^*]_{t=0}$ at $t = 0$ and $[P^*M] = [P^*M]_{t=0}$ at $t = 0$ is applied, the total concentrations of the photoexcited free and complexed pyrene sites at time t are given by

$$[P^*]_t + [P^*M]_t = A \exp(-t/\tau_1) + B \exp(-t/\tau_2) \tag{5}$$

where

$$A = [P^*M]_{t=0}\{1 - k_{-1}/(k_q - k_1[M])\} \tag{6}$$

$$B = [P^*]_{t=0}\{k_q/(k_q - k_1[M])\} \tag{7}$$

$$(1/\tau_1) = (1/\tau_0) + k_q \tag{8}$$

and

$$(1/\tau_2) = (1/\tau_0) + k_1[M] \tag{9}$$

On the other hand, under steady-state conditions, the rate equations are given by

$$d[P^*]_t/dt = \{[P]/([P] + [PM])\}I_a - (\tau_0^{-1} + k_1[M])[P^*]_t \tag{10}$$

$$d[P^*M]_t/dt = \{[PM]/([P] + [PM])\}I_a + k_1[M][P^*]_t - (\tau_0^{-1} + k_q)[P^*M]_t \tag{11}$$

where I_a is the rate of light absorption. Under steady-state conditions, $d[P^*]_t/dt = 0$ and $d[P^*M]_t/dt = 0$. Thus, the total steady-state concentrations of excited pyrenes are

$$[P^*]_s + [P^*M]_s = \{[P]/([P] + [PM])\}I_a\{(1 + K[M])(\tau_0^{-1} + k_1[M]) + k_q\}/\{(\tau_0^{-1} + k_1[M])(\tau_0^{-1} + k_q)\} \tag{12}$$

The ratio of fluorescence quantum efficiencies in the presence and absence of the quencher-carrying micelle is given by

$$\Phi/\Phi_0 = \tau_1/\tau_0 + (\tau_2/\tau_0)(1 - \tau_1/\tau_0)\{1/(1 + K[M])\} \tag{13}$$

By knowing the micelle concentration [M], one can calculate the binding constant K from steady-state fluorescence data (Φ/Φ_0) and fluorescence-decay data (τ_0, τ_1, and τ_2) via eq 13. The association rate constant k_1 and quenching rate constant k_q can be calculated from fluorescence-decay data by using eqs 9 and 8, respectively. From K and k_1, one can calculate the residence time ($1/k_{-1}$) of the micelle in the complex.

Applying the kinetic model to the steady-state and time-dependent fluorescence data in Figures 3 and 4, we calculated the association rate constants, residence times, and binding constants at $I = 0.2$. Results are plotted as a function of Y in Figure 6. For PyPAMPS the biding constant K increases by about 1 order of magnitude from 2×10^3 to 3.5×10^4 M^{-1} when Y is increased from 0.05 to 0.11. The increase in K with increasing Y can arise from both the increase in the association rate constant k_1 (Figure 6a) and the residence time $1/k_{-1}$ (Figure 6b), but the effect of Y on k_1 is more than twice its effect on $1/k_{-1}$. We conclude that fluorescence quenching for PyPAMPS at $Y < 0.04$ is due to collisional encounters, on the basis of the fact that fluorescence decays are single-exponential and that the steady-state fluorescence quenching is due to a decrease in the lifetime of fluorescence. It is to be noted that the polymer−micelle association model (Scheme 2) is only valid for cases where $Y \geq 0.05$.

The binding constant depends strongly on the hydrophobe content in PyDodPAMPS. Even when the dodecyl content is as low as 2.5 mol %, K values are more than 1 order of magnitude larger than those for PyPAMPS. As the dodecyl content is increased to 7.5 mol %, K increases by 2 orders of magnitude. This large increase in K is mainly due to a large increase in $1/k_{-1}$ with an increase in the dodecyl content (Figure 6b). The residence times for PyPAMPS

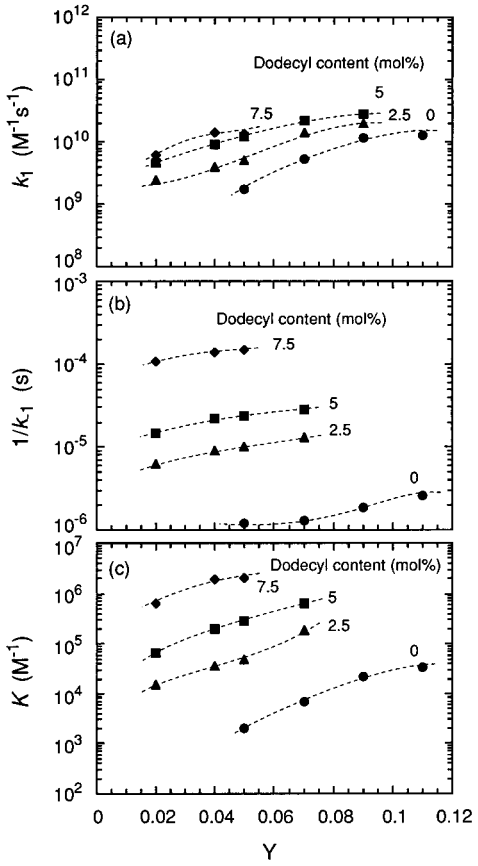

Figure 6. Association rate constant (a), residence time (b), and binding constant (c) as a function of Y for PyPAMPS and PyDodPAMPS at $I = 0.2$.

are on the order of microseconds, whereas the residence times for PyDodPAMPS (2.5 mol % dodecyl) are about 1 order of magnitude longer than those of PyPAMPS. When the dodecyl content is increased to 7.5 mol %, the residence time increases to about 100 μs, while the association rate constant k_1 shows a more modest increase (Figure 6a). Both the residence time and binding constant also depend, to a lesser degree, on the charge density of the mixed micelle, indicating the influence of electrostatic interactions.

Discussion

The ratios of the third to first vibrational fine structure (I_3/I_1) [41] in the fluorescence spectra of PyPAMPS and PyDodPAMPS in aqueous solution range from 0.59 to 0.61 regardless of dodecyl content, indicating that pyrene labels are in contact with the aqueous phase without hydrophobic association with dodecyl groups.[42] It was previously reported that random copolymers of AMPS and DodMAm formed unimolecular micelles in dilute aqueous solution, owing to intrapolymer association of dodecyl groups, when the dodecyl content exceeded ca. 30 mol %.[42] However, PyDodPAMPS employed in the present study adopts a more or less extended random coil conformation in aqueous solution, depending on ionic strength. The reduced viscosities of PyPAMPS and PyDodPAMPS at 0.1 g/dL (30 °C) range from 2 to 2.4 dL/g in pure water and from 0.2 to 0.3 dL/g in 0.1 M NaCl (molecular weights of PyPAMPS and PyDodPAMPS are on the order of 5×10^4), independent of the dodecyl content. The hydrodynamic radii (R_h) of PyPAMPS and PyDodPAMPS (7.5 mol % dodecyl concentration) in 0.1 M NaCl determined by dynamic light scattering are 7.50 and 7.55 nm, respectively. However, when the dodecyl content is increased to 10 mol %, R_h slightly decreases to 7.30 nm, while it significantly decreases to 5.35 nm when the dodecyl concentration is further increased to 20 mol %, arising from intrapolymer hydrophobic association of dodecyl groups. Therefore, it can be concluded that there is no intrapolymer hydrophobic association of dodecyl groups in PyDodPAMPS in the present study and that all hydrophobes in the polymers are available to interact with micelles; that is, each dodecyl group, and pyrene label as well, in PyDodPAMPS can interact with micelles upon encounter.

The size of $C_{12}E_6$/CTAC micelles in the absence of polymers was measured by dynamic light scattering. Over the range of compositions of interest ($0.05 < Y < 0.25$) the apparent R_h was 7.5 ± 0.2 nm, independent of Y. The extent to which the micelle aggregation number (N) may change upon binding to polymer is the subject of some debate. For the binding of dodecyltrimethylammonium bromide (DTAB) to sodium polystyrenesulfonate, Almgren et al.[43] found a 50% drop in N. On the other hand, Chu and Thomas[44] found an increase in N when decyltrimethylammonium bromide (DeTAB) binds to poly(methacrylic acid), while Thalberg et al.[45] reported no change in N when either DeTAB or DTAB binds to hyaluronic acid. Brackman and Engberts[46] reported a decrease in N when hexadecyltrimethylammonium salicylate micelles bind to the nonionic polymers poly(propylene oxide) or poly(methyl vinyl ether), but they found no change in N when the polymer was poly(ethylene oxide) or poly(vinylpyrrolidone). In the kinetic analysis of the fluorescence data in the present study, we assume that the size of $C_{12}E_6$/CTAC micelles does not change appreciably upon binding to the polymers.

As we previously reported,[35] the distribution of AMPS, dodecyl, and pyrenyl units in the polymer chain of PyDodPAMPS is completely random. Accordingly, in the case of PyPAMPS with 2.5 mol % dodecyl content, for example, each pyrene label should have a closest-neighboring dodecyl group within 20 AMPS units apart (ca. 6 nm apart if the chain is fully extended). These considerations, taken together with the size of a $C_{12}E_6$ micelle (a hydrodynamic diameter of ca. 15 nm), lead to the conceptual model for PyDodPAMPS−micelle association, depicted in Figure 7. When the micelle encounters a polymer, it may first associate with either a dodecyl or pyrene site (step 1 in Figure 7) and a "primary" complex may be formed. In step 1 in Figure 7, the dodecyl group that associates first with the micelle is not necessarily the one closest to a pyrene label. Since the diameter of the micelle (ca. 15 nm) is larger than the average distance between dodecyl and pyrene sites (maximally ca. 6 nm in the case of 2.5 mol % dodecyl concentration), neighboring pyrene and dodecyl groups may also associate with a micelle simultaneously (not illustrated in Figure 7). In the primary complex, free (uncomplexed) dodecyl or pyrene groups can readily associate with the micelle (step 2). Further associations of dodecyl groups with the micelle lead to an equilibrium complex in which a number of dodecyl groups and pyrene labels penetrate into a micelle. These processes should occur in a cooperative manner with rates much faster than the rate of step 1 because of relatively favorable entropy. Since the rate-determining step for complex formation is step 1, the association rate constant k_1 may correspond to step 1. Thus, the finding that k_1 increases with an increase in the dodecyl content is reasonable because the number of binding sites in step 1 increases with dodecyl content (the number of dodecyl sites per pyrene site is larger in polymers with higher dodecyl contents).

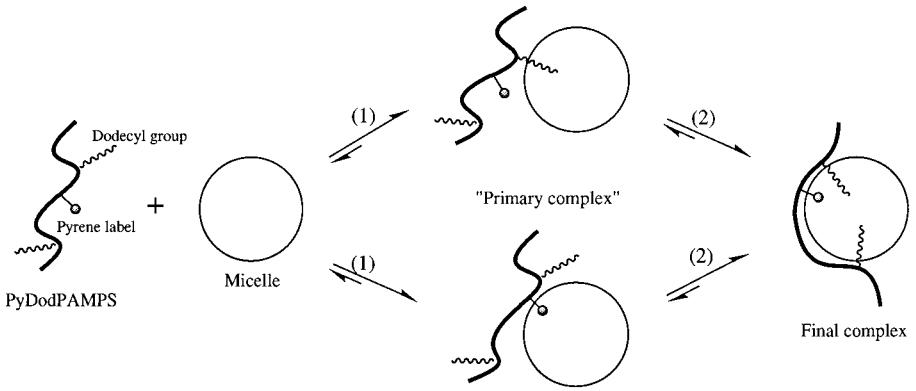

Figure 7. Conceptual model for dynamic association of PyDodPAMPS with $C_{12}E_6$/CTAC mixed micelle: (1) association step for a micelle with a dodecyl or pyrenyl group to form a "primary" complex; (2) cooperative association step for a dodecyl or pyrenyl group within the "primary" complex.

In the equilibrium complex, dodecyl groups may act as "hydrophobic anchors", holding pyrene labels tightly in the micellar phase. This situation may lead to a large increase in the residence time $1/k_{-1}$. Because the micelle is large relative to the spacing between dodecyl sites, a number of dodecyl groups can associate with a micelle for the polymers with higher dodecyl contents. Thus, the observed large increase in $1/k_{-1}$ with dodecyl content may be rationalized by an increase in the number of dodecyl anchors per pyrene label.

In the kinetic model, we assume a simple single-step equilibrium (Scheme 2). As discussed above, the association process can be represented by a single rate-determining step (step 1). On the other hand, dissociation is likely to be a multistep process, as illustrated in Figure 7. $1/k_{-1}$ represents the residence time of pyrene labels in the complex because we monitor only the quenching of pyrene fluorescence. Pyrene labels may dissociate from the equilibrium complex via reverse step 2. However, if forward step 2 occurs with a much faster rate than the rate of pyrene fluorescence (the rate constant for forward step $2 \gg 1/\tau_0$), dissociated singlet-excited pyrene labels, if any, should rapidly reenter the micelle far before they deactivate. This consideration may be reasonable because relaxation times for segment motions are on the order of subnano- or nanoseconds,[47] which is much shorter than the lifetime of pyrene fluorescence. Therefore, the observed $1/k_{-1}$ represents the residence time of the micelle in the polymer−micelle complex. In other words, k_{-1} represents the rate constant for reverse step 1 in Figure 7.

The model in Figure 7 only embodies hydrophobic associations. However, it is clear that the primary and equilibrium complexes are additionally stabilized by electrostatic interactions with an increase in Y, thus contributing to an increase in $1/k_{-1}$ as well as k_1 with increasing Y.

Conclusions

Dynamic interactions of PyPAMPS and PyDodPAMPS with mixed micelles of $C_{12}E_6$/CTAC/CPC were studied by fluorescence quenching. The binding constant (K), residence time ($1/k_{-1}$), and association rate constant (k_1) for the polymer−micelle interaction at varying mole fractions of CTAC (Y) in the mixed micelle were estimated by applying a kinetic model to steady-state and time-dependent fluorescence-quenching data. K, k_1, and $1/k_{-1}$ increase with increasing Y; k_1 is more dependent on Y than $1/k_{-1}$. Dodecyl groups in PyDodPAMPS strongly enhance the polymer−micelle interaction, leading to very large K and $1/k_{-1}$ even at small Y. Thus, the polymer−micelle association results from hydrophobic interactions between dodecyl groups and micelles with or without the conjoint action of electrostatic force.

Acknowledgment. This work was supported in part by a Grant-in-Aid for Scientific Research on Priority Areas, "New Polymers and Their Nano-Organized Systems" (No. 277/08246236), from The Ministry of Education, Science, Sports, and Culture, Japan.

References and Notes

(1) For reviews, see the following. (a) Tsuchida, E.; Abe, K. In *Interactions between Macromolecules in Solution and Intermacromolecular Complexes*; Advances in Polymer Science 45; Springer-Verlag: Berlin, 1982. (b) Smid, J.; Fish, D. *Encyclopedia of Polymer Science and Technology*; Wiley-Interscience: New York, 1988; Vol. 11, p 720.

(2) Dubin, P. L.; Rigsbee, D. R.; McQuigg, D. W. *J. Colloid Interface Sci.* **1985**, *105*, 509.

(3) McQuigg, D. W.; Kaplan, J. I.; Dubin, P. L. *J. Phys. Chem.* **1992**, *96*, 1973.

(4) Dubin, P. L.; Oteri, R. *J. Colloid Interface Sci.* **1983**, *95*, 453.

(5) Dubin, P. L.; Rigsbee, D. R.; Gan, L. M.; Fallon, M. A. *Macromolecules* **1988**, *21*, 2555.

(6) Xia, J.; Dubin, P. L.; Kim, Y. *J. Phys. Chem.* **1992**, *96*, 6805.

(7) Li, Y.; Dubin, P. L.; Dautzenberg, H.; Lück, U.; Hartmann, J.; Tuzar, Z. *Macromolecules* **1995**, *28*, 6795.

(8) Li, Y.; Xia, J.; Dubin, P. L. *Macromolecules* **1994**, *27*, 7049.

(9) Li, Y.; Dubin, P. L.; Havel, H. A.; Edwards, S. L.; Dautzenberg, H. *Macromolecules* **1995**, *28*, 3098.

(10) Xia, J.; Zhang, H.; Rigsbee, D. R.; Dubin, P. L.; Shaikh, T. *Macromolecules* **1993**, *26*, 2759.

(11) Jones, M. N. *J Colloid Interface Sci.* **1967**, *23*, 36.

(12) Rigsbee, D. R.; Dubin, P. L. *Langmuir* **1996**, *12*, 1928.

(13) Sudbeck, E. A.; Dubin, P. L.; Curran, M. E.; Skelton, J. *J. Colloid Interface Sci.* **1991**, *142*, 512.

(14) Tokiwa, F.; Tujii, K. *Bull. Chem. Soc. Jpn.* **1973**, *46*, 2684.

(15) Fishman, M. L.; Eirich, F. R. *J. Phys. Chem.* **1971**, *75*, 3135.

(16) Shirahama, K. *Colloid Polym. Sci.* **1974**, *252*, 978.

(17) Park, J. M.; Muhoberac, B. B.; Dubin, P. L.; Xia, J. *Macromolecules* **1992**, *25*, 290.

(18) Li, Y.; Dubin, P. L.; Spindles, R.; Tomalia, D. *Macromolecules* **1995**, *28*, 8426.

(19) Wiegel, F. W. *J. Phys. A: Math. Gen.* **1977**, *10*, 299.

(20) Evers, O. A.; Fleer, G. J.; Scheutjens, J. M. H. M.; Lyklema, J. *J. Colloid Interface Sci.* **1986**, *111*, 446.

(21) Muthukumar, M. *J. Chem. Phys.* **1987**, *86*, 7230.

(22) Odijk, T. *Langmuir* **1991**, *7*, 1991.

(23) von Goeler, F.; Muthukumar, M. *J. Chem. Phys.* **1994**, *100*, 7796.

(24) Muthukumar, M. *J. Chem. Phys.* **1995**, *103*, 4723.

(25) (a) Rouzima, I.; Bloomfield, V. A. *J. Phys. Chem.* **1996**, *100*, 4292. (b) Rouzima, I.; Bloomfield, V. A. *J. Phys. Chem.* **1996**, *100*, 4305.

(26) Yoshida, K.; Morishima, Y.; Dubin, P. L.; Mizusaki, M. *Macromolecules* **1997**, *30*, 6208.

(27) Mizusaki, M.; Morishima, Y.; Yoshida, K.; Dubin, P. L. *Langmuir* **1997**, *13*, 6941.

(28) See, for example, the following. (a) Abuin, E. B.; Scaiano, J. C. *J. Am. Chem. Soc.* **1984**, *106*, 6274. (b) Almgren, M.; Hansson, P.; Mukhtar, E.; van Stam J. *Langmuir* **1992**, *8*, 2405. (c) Winnik, F. M.; Winnik, M.

A.; Tazuke, S. *J. Phys. Chem.* **1987**, *91*, 594. (d) Hu, Y.; Zhao, C.; Winnik, M. A. *Langmuir* **1990**, *6*, 880.

(29) Xia, J.; Dubin, P. L.; Morishima, Y.; Sato, T.; Muhoberac, B. B. *Biopolymers* **1995**, *35*, 411.

(30) For reviews, see the following. (a) Schulz, D. N.; Bock, J.; Valint, P. L., Jr. In *Macromolecular Complexes in Chemistry and Biology*; Dubin, P., Bock, J., Davies, R. M., Schulz, D. N., Thies, C., Eds.; Springer-Verlag: Berlin Heidelberg, 1994; Chapter 1, p 3. (b) Morishima, Y. In *Multidimensional Spectroscopy of Polymers*; Urban, M. W., Provder, T., Eds.; ACS Symposium Series 598; American Chemical Society: Washington, DC, 1995; Chapter 29, p 490. (c) Morishima, Y. In *Solvents and Self-Organization of Polymers*; Webber, S. E., Munk, P., Tuzar, Z., Eds.; Kluwer Academic Publishers: Dordrecht, 1996; p 331.

(31) Winnik, F. M.; Ringsdorf, H.; Venzmer, J. *Langmuir* **1991**, *7*, 905.

(32) Goddard, E. D.; Leung, P. S. *Langmuir* **1992**, *8*, 1499.

(33) Winnik, F. M.; Regismond, S. T. A.; Goddard, E. D. *Colloids Surf.* **1996**, 243.

(34) (a) Nishikawa, T.; Akiyoshi, K.; Sunamoto, J. *Macromolecules* **1994**, *27*, 7654. (b) Akiyoshi, K.; Nishikawa, T.; Mitusi, I.; Miyata, T.; Kodama, M.; Sunamoto, J. *Colloids Surf. A.* **1996**, *112* (2/3), 91. (c) Tribet, C.; Audebert, R.; Popot, J.-L. *Langmuir*, in press.

(35) Morishima, Y.; Tominaga, Y.; Kamachi, M.; Okada, T.; Hirata, Y.; Mataga, N. *J. Phys. Chem.* **1991**, *95*, 6027.

(36) Dubin, P. L.; Thé, S. S.; Gan, L. M.; Chew, C. H. *Macromolecules* **1990**, *23*, 2500.

(37) Dubin, P. L.; Gruber, J. H.; Xia, J.; Zhang, H. *J. Colloid Interface Sci.* **1992**, *148*, 35.

(38) Chu, D.-Y.; Thomas, J. K. *Macromolecules* **1984**, *17*, 2142.

(39) Turro, N. J. In *Modern Molecular Photochemistry*; The Benjamin/Cummings Publishing: Menlo Park, CA, 1978; Chapter 9.

(40) Lianos, P.; Zana, R. *J. Colloid Interface Sci.* **1981**, *84*, 100.

(41) Kalyanasundaram, K.; Thomas, J. K. *J. Am. Chem. Soc.* **1997**, *99*, 22039.

(42) Morishima, Y.; Nomura, S.; Ikeda, T.; Seki, M.; Kamachi, M. *Macromolecules* **1995**, *28*, 2874.

(43) Almgren, M.; Hansson, P.; Mukthar, E.; van Stam, J. *Langmuir* **1992**, *8*, 2405.

(44) Chu, D.-Y.; Thomas, J. K. *J. Am. Chem. Soc.* **1986**, *108*, 6270.

(45) Thalberg, K.; van Stam, J.; Lindblad, C.; Almgren, M.; Lindman, B. *J. Phys. Chem.* **1991**, *95*, 8975.

(46) Brackman, J. C.; Engberts, J. B. F. N. *Langmuir* **1991**, *7*, 2097.

(47) Hoyle, C. H.; Nemzek, T. L.; Mar, A.; Guillet, J. E. *Macromolecules* **1978**, *11*, 429.